Original Article

Corneal densitometry changes after femtosecond laser-assisted intracorneal ring segments implantation in keratoconus

Amr Mounir [1] , Engy Mohamed Mostafa [1] , Ibrahim Amer [2] , Ahmed Abdelaleem Abdelgbar [2] , Hamdy Osman Osman [2] , Mostafa Abdelrahman Ahmed [2] , Hossam Ziada [3] , Abdel Ghany Ali El Gabbar [3] , Mohamed Alsadawy Hassan [3] and Alaa Mahmoud [1]

[1] *Ophthalmology Department, Sohag Faculty of Medicine, Sohag University, Sohag, Egypt*
[2] *Ophthalmology Department, Faculty of Medicine, Assiut branch, Al-Azhar University, Assiut, Egypt*
[3] *Ophthalmology Department, Faculty of Medicine, Cairo branch, Al-Azhar University, Cairo, Egypt*

ABSTRACT

Background: Intrastromal corneal ring segments are commonly implanted in the corneas of eyes with mild-to-moderate keratoconus; however, changes in corneal densitometry (CD) after implantation are a matter of debate in the current literature. We evaluated the changes in CD 1 and 3 months after femtosecond laser-assisted Keraring implantation.

Methods: This retrospective, non-comparative, multicenter, case series study included patients with keratoconus who underwent femtosecond laser-assisted implantation of double segments with 90° and 160° arc lengths or two 160° arc length Keraring segments. Demographic and baseline clinical ophthalmic data were recorded. Corneal topography and tomography data acquired using a Pentacam HR Scheimpflug tomography system (Pentacam High Resolution; Oculus, Wetzlar, Germany) with a best-fit sphere were used as a reference surface. Using the Pentacam HR, CD measurements were acquired over a corneal area of 12 mm in total and at four concentric zones (0–2, 2–6, 6–10, and 10–12 mm) of three corneal stromal depths: 120 μm of the anterior corneal stromal layer, 60 μm of the posterior corneal stromal layer, and the central layer of stroma lying between these two layers.

Results: We included 40 eyes of 40 patients, including 8 (20%) male and 32 (80%) female individuals, with a mean (standard deviation) age of 21.0 (6.4) years. We observed a significant improvement in the topographic values of steep keratometry (K), flat K, maximum K, and corneal astigmatism (all $P < 0.05$), but not in the mean K, thinnest corneal pachymetry, corneal thickness at the apex, back elevation, or front elevation (all $P > 0.05$). The mean total anterior, central, and posterior CD differed significantly among the time points, with a significant increase from the preoperative to the 1-month and 3-month postoperative visits (all $P < 0.05$) and no difference between those of the 1-month and 3-month postoperative visits (all $P > 0.05$). The mean CD for the anterior layer in the central, paracentral, and mid-peripheral zones, and the central layer in all four zones, differed significantly among time points, with a significant increase from the preoperative to the 1-month and 3-month postoperative visits (all $P < 0.05$), which remained unchanged from the 1-month to the 3-month postoperative visit (all $P < 0.05$), except for the central 2–6-mm zone, which decreased significantly from the 1-month to the 3-month postoperative visit ($P < 0.001$). The CD of the central 10–12-mm zone did not differ significantly in each pairwise comparison (all $P > 0.05$). In contrast, CD for the posterior layer in the paracentral zone decreased significantly from the preoperative to the 1-month and 3-month postoperative visits but increased, to a lesser extent, from the 1-month to the 3-month postoperative visit (all $P < 0.05$).

Conclusions: Femtosecond laser-assisted Keraring implantation significantly changes CD, with improvement in most topography parameters. Further longitudinal studies with larger sample sizes are required to verify these preliminary findings.

Correspondence: Amr Mounir, Ophthalmology Department, Sohag Faculty of Medicine, Sohag University, Sohag, Egypt. Email: dramrmonir@yahoo.com. ORCID iD: https://orcid.org/0000-0001-9682-671X

How to cite this article: Mounir A , Mohamed Mostafa E , Amer I, Abdelgbar AA, Osman HO , Ahmed MA , Ziada H, Ali El Gabbar AG, Hassan MA, Mahmoud A. Corneal densitometry changes after femtosecond laser-assisted intracorneal ring segments implantation in keratoconus. Med Hypothesis Discov Innov Ophthalmol. 2024 Spring; 13(1): 27-34. https://doi.org/10.51329/mehdiophthal1491

Received: : 23 March 2024; Accepted: 23 May 2024

KEYWORDS
keratoconus, pellucid marginal degeneration, densitometries, light scattering, corneas, corneal stromas, intracorneal ring segments, keraring, laser corneal surgery, femtosecond laser, corneal topographies, AI (Artificial Intelligence)

INTRODUCTION

Keratoconus (KCN) is a non-inflammatory, bilateral, asymmetric ocular disease characterized by gradual corneal thinning and steepening, resulting in irregular astigmatism and reduced visual acuity. KCN usually occurs in the second and third decades of life [1, 2]. Intracorneal ring segments (ICRSs) have been used in the management of KCN since the 2000s [3]. Various types of ICRSs exist, in which the arc length, thickness, and diameter can be chosen according to the desired effect on spherical equivalent, keratometry, and corneal sphericity. Individualized implantation strategies, based on the topographic and tomographic patterns of each patient, are constantly evolving [4].

Optical corneal densitometry (CD) refers to the value of the corneal back-scattered light and is a useful, quantitative, objective method for assessment of corneal clarity and light scattering [5, 6]. Corneal transparency is compromised in some ocular diseases, such as KCN, and the scattering of light increases with the severity of KCN [7, 8]. Backscattered light increases owing to damage to the collagen fiber arrangement and an increase in keratocyte density in the central parts of corneas with KCN [8]. Pentacam HR evaluates the optical CD in the range of 0 (minimum scattering) to 100 (maximum scattering) in the grayscale units (GSUs) criterion using Scheimpflug imaging technology, and it provides a map of the posterior scattered light [9].

Currently, intrastromal corneal ring segments (ICRSs) are commonly used to treat mild-to-moderate KCN in the absence of a central corneal scar and in patients with contact lens intolerance [10]. ICRSs decrease the spherocylindrical refractive error by reducing the corneal curvature and diminishing higher-order aberrations to increase corneal regularity [11]. Implanting ICRSs in the corneal mid-periphery creates a flattening effect in the central cornea [12], changes the corneal curvature toward normal status, and improves uncorrected and best-corrected visual acuities [13].

Femtosecond laser technology allows the surgeon to program a corneal stromal dissection at a predetermined depth with an exceptionally high degree of accuracy. This avoids the potential inaccuracies of a mechanical dissection, which are dependent on the surgeon's manual skills [14]. The use of femtosecond lasers for ICRS tunnel creation has been widely accepted since their FDA approval. Tunnels can be created at 70–80% of the corneal thickness within 15 s with less manipulation. The device delivers adjacent laser pulses at a predetermined depth in the stroma. This creates an extended bubble of gas and water to dissect the tissue and form a plane of separation and a tunnel for ICRS implantation [15]. However, the effects of femtosecond laser technology on CD have been debated in the literature [16, 17].

We evaluated changes in corneal topography and densitometry in eyes with KCN after femtosecond laser-assisted ICRS implantation.

METHODS

This retrospective, non-comparative, multicenter, case series study was conducted between January 2022 and January 2023 at three centers in Egypt: the Center for Corneal and Refractive Surgeries in Sohag City, the Tiba Refractive Center in Assiut City, and the I-Vision Eye Hospital in Cairo. This study was approved by the Ethics Committee of the Sohag Faculty of Medicine, Sohag University, Sohag, Egypt (approval number IBR #Soh-Med-24-02-06PD) and followed the tenets of the Declaration of Helsinki. Adult participants provided written informed consent for participation in this study, and parents or legal guardians provided consent for patients under 18 years of age.

The study included all eligible eyes with KCN [18, 19] and contact lens intolerance that underwent femtosecond laser-assisted ICRS implantation [17, 20, 21] with a 3-month postoperative follow-up. We excluded eyes with previous ocular surgery or trauma, corneal opacity, or pellucid marginal degeneration; individuals with connective tissue diseases; and pregnant or breastfeeding women.

Demographic and baseline clinical ophthalmic data were recorded, including uncorrected distance visual acuity (UDVA) and best-corrected distance visual acuity (BCDVA) using an Auto Chart Projector (CP 670; Nidek Co., Ltd., Gamagori, Japan), with values recorded in logarithm of the minimum angle of resolution (logMAR) notation; manifest and cycloplegic refractions after instilling cyclopentolate 1% eye drops (Swixolate, Chemipharm Pharmaceutical Industries, Cairo, Egypt) using an auto-refractometer (HUVITZ HRK-7000A; Huvitz, Gunpo, South Korea); detailed anterior segment and dilated posterior segment examinations under a slit lamp (Haag-Streit Slit Lamp BX 900; Haag-Streit, Koeniz, Switzerland); and intraocular pressure measurement using Goldmann applanation tonometry (BP 900®, Haag-Streit).

The Pentacam HR Scheimpflug system (Oculus Optikgerate GmbH, Wetzlar, Germany), with a best-fit sphere as a reference surface, was used to acquire keratometry (K) values in diopters (steep K, flat K, mean K, and maximum K); corneal astigmatism in diopter cylinders (DC); thinnest corneal pachymetry (TCP) and corneal thickness at the apex (pachy apex) in µm; and front and back elevation in µm [22, 23] at baseline and two postoperative visits.

Using the Pentacam HR Scheimpflug system, CD measurements were acquired at baseline and at two postoperative visits in a dark room by one physician in each participating center. The standardized Scheimpflug densitometry is represented in GSUs. The device software assesses the CD over a corneal area of 12 mm in total and at four concentric zones (0–2, 2–6, 6–10, and 10–12 mm) of three corneal stromal depths: 120 µm of the anterior corneal stromal layer, 60 µm of the posterior corneal stromal layer, and the central layer of stroma lying between these two layers [17]. All eyes underwent implantation of double segment 90° and 160° arc length Keraring or two 160° arc length Keraring segments (Keraring ICRS; Mediphacos Ltd., Belo Horizonte, Brazil) through an intrastromal tunnel. Ring parameters were selected based on the manufacturer's nomogram [24]. Surgeries were performed using the IntraLase® IFS femtosecond 150-Hz laser (Johnson & Johnson, New Brunswick, NJ, USA) [17], and the corneal incision depth was 80% of the thinnest point in the tunnel path, with an optical zone of 5 mm, an inner diameter of 5.1 mm, and an outer diameter of 5.9 mm [20]. All eyes received similar topical medications postoperatively [21]. Preoperative and 1- and 3-month postoperative tomography, topography, and densitometry measurements were obtained for all the included eyes (Figure 1).

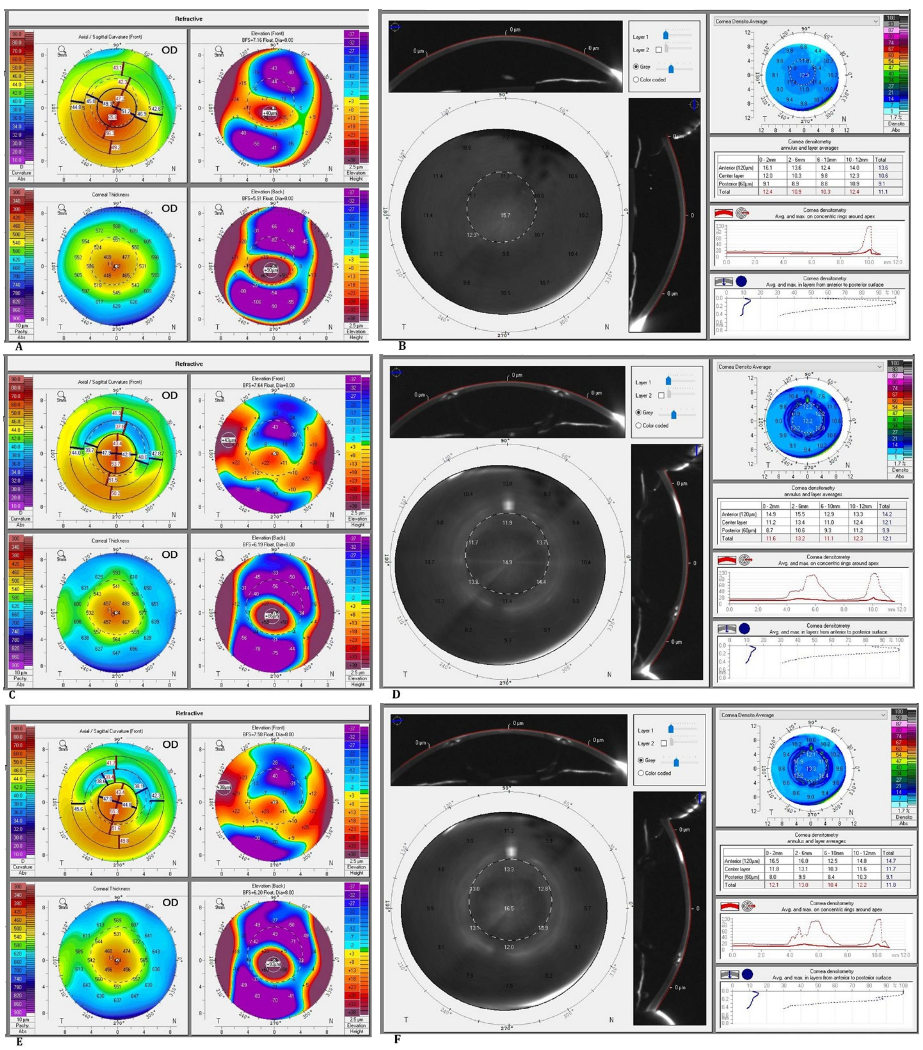

Figure 1. Right eye preoperative (A, B), 1-month (C, D), and 3-month (E, F) postoperative corneal topography (A, C, E) and densitometry (B, D, F) images using the Pentacam HR Scheimpflug system (Oculus Optikgerate GmbH, Wetzlar, Germany) of a representative case with keratoconus who underwent femtosecond laser-assisted intracorneal ring segment implantation. Corneal optical densitometry displays the position (D, F) and depth of two Keraring intrastromal corneal ring segments (Keraring ICRS; Mediphacos Ltd., Belo Horizonte, Brazil).

Statistical analysis was performed using SigmaStat software (SigmaStat 4.0, Systat Software Inc., Chicago, IL, USA). Normality of the data distribution was analyzed using the Kolmogorov–Smirnov test. Quantitative and qualitative variables are reported as mean (standard deviation [SD]) and frequency (%), respectively. Differences across the three time points were evaluated using one-way repeated-measures analysis of variance (ANOVA), and if significance was found, a post-hoc analysis using Tukey's test was used for pairwise comparisons. A *P*-value < 0.05 was considered to indicate a statistically significant difference.

RESULTS

We included 40 eyes of 40 patients with a mean (SD) age of 21.0 (6.4) years, including 8 (20%) male and 32 (80%) female individuals. Table 1 summarizes the baseline demographic and clinical characteristics of the participants, and Table 2 summarizes the tomography, topography, and densitometry values of the participants at baseline and the two postoperative visits.

The mean (SD) values for steep K, flat K, maximum K, and corneal astigmatism differed significantly among the time points (all $P < 0.001$); however, the mean (SD) values for mean K, TCP, pachy apex, back elevation, and front elevation did not (all $P > 0.05$) (Table 2). Pairwise comparisons revealed that steep K, flat K, maximum K, and corneal astigmatism decreased significantly from the preoperative to the 1-month postoperative visit, from the preoperative to the 3-month postoperative visit, and from the 1-month to the 3-month postoperative visit (all $P < 0.05$), except for corneal astigmatism at the 3-month visit, which was significantly higher than that of the 1-month visit ($P < 0.001$), and maximum K at the 1-month visit, which did not differ significantly from the baseline value ($P > 0.05$) (Table 2).

The mean (SD) values for total anterior CD and CD of the 0–2-, 2–6-, and 6–10-mm concentric annular zones differed significantly among the time points (all $P < 0.001$); however, the mean CD of the anterior 10–12-mm zone did not ($P > 0.05$). Pairwise comparisons revealed that the anterior CD in total and in the 0–2-, 2–6-, and 6–10-mm concentric annular zones increased significantly from the preoperative to the 1-month and 3-month postoperative visits (all $P < 0.001$) but remained unchanged from the 1-month to the 3-month postoperative visit (all $P > 0.05$) (Table 2).

The mean (SD) values for the total central CD and the CD of all four concentric annular zones in the central layer differed significantly among the time points (all $P < 0.001$). Pairwise comparisons revealed that the central CD in total and in all four concentric annular zones at the central layer increased significantly from the preoperative to the 1-month and 3-month postoperative visits (all $P < 0.001$) and remained unchanged from the 1-month to the 3-month postoperative visit (all $P > 0.05$), except for the central 2–6-mm zone, which decreased significantly from the 1-month to the 3-month postoperative visit ($P < 0.001$), and the mean CD of the central 10–12-mm zone, which did not differ significantly in each pairwise comparison (all $P > 0.05$) (Table 2).

The mean (SD) values for the total posterior CD and the CD of the 2–6-mm concentric annular zone differed significantly among time points (both $P < 0.001$); however, the CD of the posterior 0–2-, 6–10-, and 10–12-mm concentric annular zones did not (all $P > 0.05$). Pairwise comparisons revealed that total posterior CD increased significantly from the preoperative to the 1-month and the 3-month postoperative visits (both $P < 0.001$) but remained unchanged from the 1-month to the 3-month postoperative visit ($P > 0.05$). In contrast, posterior CD in the 2–6-mm concentric annular zone decreased significantly from the preoperative to the 1-month and the 3-month postoperative visits (both $P < 0.001$) but increased significantly, to a lesser degree, from the 1-month to the 3-month postoperative visit ($P < 0.05$) (Table 2).

Table 1. Baseline characteristics of the study participants

Variable	Value
Age (y), Mean ± SD	21.0 ± 6.4
Sex (Male / Female), n (%)	8 (20) / 32 (80)
Laterality (Right eye / Left eye), n (%)	25 (62.5) / 15 (37.5)
UCDVA (logMAR), Mean ± SD	0.31 ± 0.20
BCDVA (logMAR), Mean ± SD	0.15 ± 0.02
SEQ (D), Mean ± SD	- 9.2 ± 5.5
IOP (mmHg), Mean ± SD	13.0 ± 5.0
Q-value, Mean ± SD	- 2.0 ± 0.3

Abbreviations: y, years; SD, standard deviation; n, number of patients; %, percentage; UCDVA, uncorrected distance visual acuity; logMAR, logarithm of the minimum angle of resolution; BCDVA, best-corrected distance visual acuity; SEQ, spherical equivalent of refractive error calculated as the spherical component of the refractive error + 1/2 the cylindrical component; D, diopters; IOP, intraocular pressure; mmHg, millimeter of mercury; Q-value, corneal asphericity coefficient.

Table 2. Preoperative and postoperative corneal tomography, topography, and densitometry data

Variable	Preoperative, Mean ± SD	1-month post-op, Mean ± SD	3-month post-op, Mean ± SD	P_1	Pairwise comparisons P_2	P_3	P_4
Steep K (D)	56.0 ± 12.7	50.2 ± 4.5	49.2 ± 4.7	**< 0.001**	**< 0.001**	**< 0.001**	**< 0.001**
Flat K (D)	50.8 ± 4.1	47.8 ± 4.2	47.3 ± 4.3	**< 0.001**	**< 0.001**	**< 0.001**	**< 0.001**
Mean K (D)	53.1 ± 12.0	48.9 ± 4.2	48.2 ± 4.3	0.33	-	-	-
K max (D)	67.0 ± 7.5	64.7 ± 8.9	63.8 ± 8.6	**< 0.001**	0.24	**0.007**	**0.003**
Corneal astigmatism (DC)	5.1 ± 2.0	2.5 ± 1.3	2.7 ± 1.7	**< 0.001**	**< 0.001**	**< 0.001**	**0.01**
TCP (µm)	434.0 ± 32.0	455.8 ± 44.2	439.7 ± 34.0	0.07	-	-	-
Pachy apex (µm)	439.3 ± 34.7	463.8 ± 47.6	447.0 ± 40.0	0.04	-	-	-
Back elevation (µm)	72.0 ± 24.2	83.9 ± 22.7	80.4 ± 24.7	0.13	-	-	-
Front elevation (µm)	36.0 ± 9.5	37.0 ± 9.5	37.0 ± 10.7	0.9	-	-	-
CD anterior 0–2 mm (GSU)	16.7 ± 1.4	19.0 ± 3.1	24.8 ± 26.7	**< 0.001**	**< 0.002**	**< 0.003**	0.5
CD anterior 2–6 mm (GSU)	13.9 ± 1.1	16.3 ± 2.8	16.3 ± 2.6	**< 0.001**	**< 0.001**	**< 0.001**	0.05
CD anterior 6–10 mm (GSU)	13.6 ± 3.2	14.6 ± 2.6	14.8 ± 2.7	**< 0.001**	**< 0.001**	**< 0.001**	0.3
CD anterior 10–12 mm (GSU)	31.8 ± 16.3	35.1 ± 13.0	34.8 ± 12.6	0.3	-	-	-
CD anterior total (GSU)	16.3 ± 2.7	20.0 ± 5.6	19.8 ± 5.5	**< 0.001**	**< 0.001**	**< 0.001**	0.24
CD central 0–2 mm (GSU)	11.7 ± 0.7	12.4 ± 1.4	12.7 ± 1.5	**< 0.001**	**< 0.001**	**< 0.001**	0.24
CD central 2–6 mm (GSU)	10.4 ± 0.6	13.5 ± 1.3	13.4 ± 2.6	**< 0.001**	**< 0.001**	**< 0.001**	**< 0.001**
CD central 6–10 mm (GSU)	10.3 ± 1.6	11.0 ± 0.9	11.2 ± 1.2	**< 0.001**	**< 0.001**	**< 0.001**	0.98
CD central 10–12 mm (GSU)	21.3 ± 9.7	22.9 ± 7.3	22.5 ± 7.5	**< 0.001**	0.83	0.9	0.3
CD central total (GSU)	11.9 ±1.5	13.6 ± 1.1	13.8 ± 0.8	**< 0.001**	**< 0.001**	**< 0.001**	0.2
CD posterior 0–2 mm (GSU)	8.8 ± 0.5	8.6 ± 0.9	8.9 ± 1.1	0.23	-	-	-
CD posterior 2–6 mm (GSU)	12.4 ±16.2	9.8 ± 0.8	10.0 ± 0.7	**< 0.001**	**< 0.001**	**< 0.001**	**0.01**
CD posterior 6–10 mm (GSU)	8.6 ± 0.9	8.8 ± 0.6	9.0 ± 1.1	0.4	-	-	-
CD posterior 10–12 mm (GSU)	14.8 ± 4.1	15.5 ± 4.1	15.6 ± 4.7	0.7	-	-	-
CD posterior total (GSU)	9.4 ± 0.8	10.0 ± 0.7	10.0 ± 0.8	**< 0.001**	**< 0.001**	**< 0.001**	0.6

Abbreviations: Post-op, post-operative; SD, standard deviation; K, keratometry reading; D, diopters; DC, diopters cylinder; TCP, thinnest corneal pachymetry; µm, micrometer; Pachy apex, corneal thickness at the apex; CD, corneal densitometry; mm, millimeters; GSU, grayscale units. Note: P_1: Compares the three values across the preoperative, 1-month postoperative, and 3-month postoperative visits using one-way repeated-measures analysis of variance (ANOVA); P_2, P_3, and P_4: *P*-values are derived from pairwise comparisons using post-hoc Tukey's test in which P_2 compares preoperative values with those of the 1-month postoperative visit, P_3 compares preoperative values with those of the 3-month postoperative visit, and P_4 compares the values at the 1-month versus the 3-month postoperative visit.

DISCUSSION

We observed a significant improvement in the topographic values of steep K, flat K, maximum K, and corneal astigmatism, but not in the mean K, TCP, pachy apex, back elevation, or front elevation in eyes with KCN after femtosecond laser-assisted ICRS implantation in short-term follow-up. The mean total anterior, central, and posterior CD differed significantly among the time points, with a significant increase from the preoperative to the 1-month and 3-month postoperative visits and no significant difference from the 1-month to the 3-month postoperative visit. Concerning central (0–2-mm annulus), paracentral (2–6-mm annulus), mid-peripheral (6–10-mm annulus) [25], and peripheral (10–12-mm annulus) [26] zones, CD for the anterior layer in the central, paracentral, and mid-peripheral zones and for the central layer in all four zones differed significantly among time points, with a significant increase from the preoperative to the 1-month and 3-month postoperative visits, and no change from the 1-month to the 3-month postoperative visit, except for the central 2–6-mm zone, in which CD decreased significantly from the 1-month to the 3-month postoperative visit, and the central 10–12-mm zone, in which CD did not differ significantly in each pairwise comparison. In contrast, CD for the posterior layer in the paracentral zone decreased significantly from the preoperative to the 1-month and 3-month postoperative visits but increased significantly, to a lesser extent, from the 1-month to the 3-month postoperative visit.

Optical CD is evaluated non-invasively using a Scheimpflug camera, which measures light transmission through the corneal tissue and quantifies backward dispersion [27]. Changes in fibrillar regulation or orientation, such as the loss of parallel arrangement or interlacing and a reduction of the stromal lamellar portion seen in KCN, may lead to a reduction in corneal transparency [28-30]. This increases light backscattering in the central portion of eyes with KCN than in those with a normal cornea [31]. In advanced cases of ectasia, lamellar derangement may lead to scarring with an evident reduction in corneal transparency [30]. We evaluated short-term changes in CD after femtosecond laser-assisted ICRS implantation in 40 eyes with KCN using Pentacam measurements of backward light scattering.

Studies have evaluated CD changes in eyes with KCN [32, 33]; however, our study evaluated the effect of femtosecond laser-assisted ICRS implantation on CD. Comparison of the CD of the three corneal layers over the four circular annuli revealed a significant increase in total CD after surgery in all three layers of the cornea—anterior, central, and posterior. These results corroborate those of Sedaghat et al. [16], who investigated changes in corneal backscattering using a Pentacam 6 months after Keraring implantation for KCN. They found a significant increase in CD, mainly in the anterior paracentral cornea (2–6-mm annulus), for all layers associated with the position of the ring implant [16].

Basiony et al. [27] investigated CD changes in various annuli and depths in the corneas of patients with KCN who underwent femtosecond laser-assisted Keraring implantation in multiple follow-ups during a 3-month period and found significant changes in CD, mainly in the central corneal layer and in the 2–6-mm annular zone, with a reverse correlation with keratometric values of the front corneal surface. CD in the peripheral zone of 10–12 mm in the anterior and central layers remained unchanged and decreased significantly in the posterior layer [27]. In our study, CD in the peripheral zone of 10–12 mm in all layers was similar in all comparisons, whereas CD significantly increased in the central zones of 0–2 mm in the anterior and central layers. This can be explained by the absence of peripheral corneal clarity changes in eyes with KCN compared to healthy control eyes [34].

Mathews et al. [35] and Pircher et al. [36] observed increased CD with corneal flattening after crosslinking in eyes with progressive KCN. We observed a significant increase in CD with a significant flattening of steep, flat, and maximum K values, corroborating the findings of studies attributing increasing CD to the flattening effect of Keraring implantation [16, 27]. In contrast, Alzahrani and colleagues found no statistically significant change in CD after implantation of Intacs at 12 months post-treatment [37]. This can be explained by the significant differences between the types of implanted rings, Intacs [37] versus Keraring [16, 27], with their different shapes and sites of implantation. Intacs is implanted more peripherally [38], with an elliptical cross-section and inner diameter of 6.77 mm, whereas Keraring has a triangular cross-section [38] and a smaller inner diameter [39]. However, further comparative studies are required to validate our reasoning.

Using Pentacam and a similar follow-up period, Rodrigues et al. [17] observed decreased CD of the central 0–2-mm zone attributable to regularization of the corneal lamellae in the optical zone [17]. Although CD was measured in four annular zones, as in our study, the CD data of the central 0–2-mm zone of the two anterior and central layers were analyzed [17]. In contrast with our study, which observed a possible trend in changing CD through two postoperative visits, Rodrigues et al. [17] assessed the correlation between preoperative and 3-month postoperative CD; however, K values and mean CD values were not reported [17]. Considering the differences in aim and statistical analysis between the two studies, a direct comparison of the results is not possible.

Jabbervand et al. [40] studied CD changes in eyes with KCN 12 months after implantation of an annular intracorneal inlay (AICI). They observed a significant increase in CD of the central layer in total and in the 0–2-, 2–6-, and 6–10-mm annular zones; in the total 2–6-mm zone; and in the 2–6-mm zone of the posterior layer, with a significant decrease in CD of the 0–2-mm anterior ring. However, CD remained unchanged in the 0–2-mm zone in the total and posterior layers; in the 2–6-mm zone in the anterior layer; in the 6–10-mm zone in the anterior layer, posterior layer, and total cornea; in the 10–12-mm zone of all three layers and total cornea; and in the total CD in the anterior, posterior, and total cornea [40]. This indicates that intracorneal implants, regardless of implant type and depth, could affect CD parameters to some extent.

This study assessed short-term changes in CD and topography parameters after femtosecond laser-assisted Keraring implantation in eyes with KCN. However, our study has certain limitations. A skewed male-to-female ratio was observed, which should be avoided in future studies. Furthermore, different factors can affect corneal backscattering after Keraring implantation, including a significant reduction in anterior chamber depth after the ICRS implantation [41, 42]; another factor is iris color, which influences backscattering of light after surgery [43]. However, we did not evaluate these parameters in this study. Further studies are needed to evaluate the different factors causing increased densitometry values after ICRS implantation, and to determine possible correlations between these factors and CD. Artificial intelligence could optimize the management outcomes of potentially blinding ocular conditions, including KCN. A better functional outcome was reported using an artificial neural network than using the manufacturer's nomograms after femtosecond laser-assisted Keraring implantation in eyes with KCN [44]. Therefore, studies on the moderating role of artificial intelligence for implanting ICRSs and the increases in postoperative CD may be an exciting and highly creative topic for further research.

CONCLUSIONS

Femtosecond laser-assisted Keraring implantation leads to significant changes in CD. We observed significant improvements in most topographic parameters. The mean total CD in all three corneal layers increased significantly from the preoperative to the 1-month and 3-month postoperative visits. Likewise, CD for the anterior layer in the central, paracentral, and mid-peripheral zones and for the central layer in all four zones changed significantly from the preoperative to the 1-month and 3-month postoperative visits. In contrast, CD for the posterior layer in the paracentral zone decreased significantly from the preoperative to the 1-month and 3-month postoperative visits but increased significantly, to a lesser extent, from the 1-month to the 3-month postoperative visit. Further longitudinal studies with larger sample sizes are required to verify these preliminary findings.

ETHICAL DECLARATIONS

Ethical approval: This study was approved by the Ethics Committee of the Sohag Faculty of Medicine, Sohag University, Sohag, Egypt (approval number IBR #Soh-Med-24-02-06PD) and followed the tenets of the Declaration of Helsinki. Adult participants provided written informed consent for participation in this study, and parents or legal guardians provided consent for patients under 18 years of age.
Conflict of interest: None.

FUNDING

None.

ACKNOWLEDGMENTS

None.

REFERENCES

1. Santodomingo-Rubido J, Carracedo G, Suzaki A, Villa-Collar C, Vincent SJ, Wolffsohn JS. Keratoconus: An updated review. Cont Lens Anterior Eye. 2022;45(3):101559. doi: 10.1016/j.clae.2021.101559 pmid: 34991971
2. Iqbal M, Hammour A, Elsayed A, Gad A. Outcomes of the Q value-based nomogram in managing pediatric versus adult keratoconus: a prospective interventional study. Med Hypothesis Discov Innov Ophthalmol. 2023;12(2):78-89. doi: 10.51329/mehdiophthal1473 pmid: 38357612
3. Colin J, Cochener B, Savary G, Malet F. Correcting keratoconus with intracorneal rings. J Cataract Refract Surg. 2000;26(8):1117-22. doi: 10.1016/s0886-3350(00)00451-x pmid: 11008037
4. David C, Kallel S, Trinh L, Goemaere I, Borderie V, Bouheraoua N. Les anneaux intra-cornéens dans la prise en charge du kératocône [Intracorneal ring segments in keratoconus management]. J Fr Ophtalmol. 2021;44(6):882-898. French. doi: 10.1016/j.jfo.2020.10.021 pmid: 33895029
5. Wegener A, Laser-Junga H. Photography of the anterior eye segment according to Scheimpflug's principle: options and limitations - a review. Clin Exp Ophthalmol. 2009;37(1):144-54. doi: 10.1111/j.1442-9071.2009.02018.x pmid: 19338611
6. Shen Y, Han T, Jhanji V, Shang J, Zhao J, Li M, et al. Correlation Between Corneal Topographic, Densitometry, and Biomechanical Parameters in Keratoconus Eyes. Transl Vis Sci Technol. 2019;8(3):12. doi: 10.1167/tvst.8.3.12 pmid: 31110913
7. Dong J, Zhang Y, Zhang H, Jia Z, Zhang S, Sun B, et al. Corneal densitometry in high myopia. BMC Ophthalmol. 2018;18(1):182. doi: 10.1186/s12886-018-0851-x pmid: 30045701
8. Koc M, Tekin K, Tekin MI, Uzel MM, Kosekahya P, Ozulken K, et al. An Early Finding of Keratoconus: Increase in Corneal Densitometry. Cornea. 2018;37(5):580-586. doi: 10.1097/ICO.0000000000001537 pmid: 29384807
9. Shen Y, Jian W, Sun L, Li M, Han T, Son J, et al. One-Year Follow-Up of Changes in Corneal Densitometry After Accelerated (45 mW/cm2) Transepithelial Corneal Collagen Cross-Linking for Keratoconus: A Retrospective Study. Cornea. 2016;35(11):1434-1440. doi: 10.1097/ICO.0000000000000934 pmid: 27429089
10. Ibrahim O, Elmassry A, Said A, Abdalla M, El Hennawi H, Osman I. Combined femtosecond laser-assisted intracorneal ring segment implantation and corneal collagen cross-linking for correction of keratoconus. Clin Ophthalmol. 2016;10:521-6. doi: 10.2147/OPTH.S97158 pmid: 27041991
11. Hosny M, El-Mayah E, Sidky MK, Anis M. Femtosecond laser-assisted implantation of complete versus incomplete rings for keratoconus treatment. Clin Ophthalmol. 2015;9:121-7. doi: 10.2147/OPTH.S73855 pmid: 25657576
12. Coskunseven E, Kymionis GD, Tsiklis NS, Atun S, Arslan E, Siganos CS, et al. Complications of intrastromal corneal ring segment implantation using a femtosecond laser for channel creation: a survey of 850 eyes with keratoconus. Acta Ophthalmol. 2011;89(1):54-7. doi: 10.1111/j.1755-3768.2009.01605.x pmid: 19681760
13. Sakellaris D, Balidis M, Gorou O, Szentmary N, Alexoudis A, Grieshaber MC, et al. Intracorneal Ring Segment Implantation in the Management of Keratoconus: An Evidence-Based Approach. Ophthalmol Ther. 2019;8(Suppl 1):5-14. doi: 10.1007/s40123-019-00211-2 pmid: 31605316
14. Piñero DP, Alio JL, El Kady B, Coskunseven E, Morbelli H, Uceda-Montanes A, et al. Refractive and aberrometric outcomes of intracorneal ring segments for keratoconus: mechanical versus femtosecond-assisted procedures. Ophthalmology. 2009;116(9):1675-87. doi: 10.1016/j.ophtha.2009.05.016 pmid: 19643498
15. El-Sebaey AE, Nagy AM, Farid FM. Evaluation of femtosecond laser-assisted implantation of intracorneal ring segments in cases of keratoconus. Menoufia Medical Journal. 2019;32(1):375-9. doi: 10.4103/mmj.mmj_45_18
16. Sedaghat MR, Momeni-Moghaddam H, Heravian J, Belin MW, Ambrósio R Jr, Gheysari-Alishahi T, et al. Scheimpflug Corneal Densitometry Changes After the Intrastromal Corneal Ring Segment Implantation. Cornea. 2020;39(6):761-768. doi: 10.1097/ICO.0000000000002307 pmid: 32195751
17. Rodrigues PF, Moscovici BK, Ferrara G, Lamazales L, Freitas MMS, Torquetti L, et al. Corneal densitometry in patients with keratoconus undergoing intrastromal Ferrara ring implantation. Eur J Ophthalmol. 2021;31(6):3505-3510. doi: 10.1177/11206721211020631 pmid: 34058904
18. Song M, Chen T, Moktar A, Chan E, Chong EW, Daniell M, et al. Diagnosis and Management of Keratoconus-A Narrative Review of Clinicians' Perspectives. Children (Basel). 2022;9(12):1973. doi: 10.3390/children9121973 pmid: 36553416
19. Mounir A, El Saman IS, Anbar M. The Correlation between Corneal Topographic Indices and Corneal High Order Aberrations in Keratoconus. Med Hypothesis Discov Innov Ophthalmol. 2019;8(1):1-6. pmid: 30923715

20. Gharaibeh AM, Muhsen SM, AbuKhader IB, Ababneh OH, Abu-Ameerh MA, Albdour MD. KeraRing intrastromal corneal ring segments for correction of keratoconus. Cornea. 2012;31(2):115-20. doi: 10.1097/ICO.0b013e3182215a15 pmid: 22146550
21. Mounir A, Radwan G, Farouk MM, Mostafa EM. Femtosecond-assisted intracorneal ring segment complications in keratoconus: from novelty to expertise. Clin Ophthalmol. 2018;12:957-964. doi: 10.2147/OPTH.S166538 pmid: 29872254
22. de Sanctis U, Loiacono C, Richiardi L, Turco D, Mutani B, Grignolo FM. Sensitivity and specificity of posterior corneal elevation measured by Pentacam in discriminating keratoconus/subclinical keratoconus. Ophthalmology. 2008;115(9):1534-9. doi: 10.1016/j.ophtha.2008.02.020 pmid: 18405974
23. Ruiseñor Vázquez PR, Galletti JD, Minguez N, Delrivo M, Fuentes Bonthoux F, Pförtner T, et al. Pentacam Scheimpflug tomography findings in topographically normal patients and subclinical keratoconus cases. Am J Ophthalmol. 2014;158(1):32-40.e2. doi: 10.1016/j.ajo.2014.03.018 pmid: 24709808
24. Rocha G, Silva LNP, Chaves LFOB, Bertino P, Torquetti L, de Sousa LB. Intracorneal Ring Segments Implantation Outcomes Using Two Different Manufacturers' Nomograms for Keratoconus Surgery. J Refract Surg. 2019;35(10):673-683. doi: 10.3928/1081597X-20190916-01 pmid: 31610009
25. Lazaridis A, Giallouros E, Sekundo W, Schroeder FM, Sklavos S, Droutsas K. Spatial Analysis of Corneal Densitometry, Thickness Profile, and Volume Distribution After Uneventful Descemet Membrane Endothelial Keratoplasty. Cornea. 2019;38(10):1215-1221. doi: 10.1097/ICO.0000000000002035 pmid: 31306285
26. Droutsas K, Kappos N, Giallouros E, Schroeder FM, Sekundo W, Kandarakis S, et al. Corneal Densitometry After Uneventful Descemet Membrane Endothelial Keratoplasty-5-Year Outcomes. Cornea. 2022;41(8):1002-1008. doi: 10.1097/ICO.0000000000002919 pmid: 34839334
27. Basiony AI, Abdulfattah MM, Ibrahim AM. Corneal densitometry changes in keratoconus patients after intrastromal corneal ring segments implantation. Journal of the Egyptian Ophthalmological Society. 2024;117(1):28-38. doi: 10.4103/ejos.ejos_55_23
28. Meek KM, Knupp C. Corneal structure and transparency. Prog Retin Eye Res. 2015;49:1-16. doi: 10.1016/j.preteyeres.2015.07.001 pmid: 26145225
29. Meek KM, Tuft SJ, Huang Y, Gill PS, Hayes S, Newton RH, et al. Changes in collagen orientation and distribution in keratoconus corneas. Invest Ophthalmol Vis Sci. 2005;46(6):1948-56. doi: 10.1167/iovs.04-1253 pmid: 15914608
30. Morishige N, Wahlert AJ, Kenney MC, Brown DJ, Kawamoto K, Chikama T, et al. Second-harmonic imaging microscopy of normal human and keratoconus cornea. Invest Ophthalmol Vis Sci. 2007;48(3):1087-94. doi: 10.1167/iovs.06-1177 pmid: 17325150
31. Lopes B, Ramos I, Ambrósio R Jr. Corneal densitometry in keratoconus. Cornea. 2014;33(12):1282-6. doi: 10.1097/ICO.0000000000000266 pmid: 25285589
32. Mounir A, Awny I, Yousef HS, Mostafa EM. Distribution of corneal densitometry in different grades of keratoconus. Indian J Ophthalmol. 2023;71(3):830-836. doi: 10.4103/ijo.IJO_1792_22 pmid: 36872687
33. Alnawaiseh M, Eter N. Korneale Densitometrie : Stellenwert in der Keratokonusdiagnostik [Corneal densitometry : Value for keratoconus diagnostics]. Ophthalmologe. 2018;115(9):737-743. German. doi: 10.1007/s00347-018-0667-3 pmid: 29468296
34. Anayol MA, Sekeroglu MA, Ceran BB, Dogan M, Gunaydin S, Yilmazbas P. Quantitative assessment of corneal clarity in keratoconus: a case control study of corneal densitometry. Eur J Ophthalmol. 2016;26(1):18-23. doi: 10.5301/ejo.5000644 pmid: 26165332
35. Mathews PM, De Rojas JO, Rapuano PB, Zemsky CJ, Florakis GJ, Trokel SL, et al. Correlation of Scheimpflug densitometry changes with clinical outcomes after corneal crosslinking. J Cataract Refract Surg. 2018;44(8):993-1002. doi: 10.1016/j.jcrs.2018.05.016 pmid: 30115299
36. Pircher N, Pachala M, Prager F, Pieh S, Schmidinger G. Changes in straylight and densitometry values after corneal collagen crosslinking. J Cataract Refract Surg. 2015;41(5):1038-43. doi: 10.1016/j.jcrs.2014.07.043 pmid: 25953473
37. Alzahrani K, Cristian C, Harper S, Carley F, Brahma A, Morley D, et al. Corneal imaging and densitometry measurements in keratoconus patients to monitor disease progression and treatment outcomes after contact lens or Intacs treatment. Clin Ophthalmol. 2018;12:1653-1658. doi: 10.2147/OPTH.S168865 pmid: 30233127
38. Alfonso JF, Lisa C, Fernández-Vega L, Madrid-Costa D, Montés-Micó R. Intrastromal corneal ring segment implantation in 219 keratoconic eyes at different stages. Graefes Arch Clin Exp Ophthalmol. 2011;249(11):1705-12. doi: 10.1007/s00417-011-1759-9 pmid: 21842130
39. Piñero DP, Alio JL, Teus MA, Barraquer RI, Uceda-Montañés A. Modeling the intracorneal ring segment effect in keratoconus using refractive, keratometric, and corneal aberrometric data. Invest Ophthalmol Vis Sci. 2010;51(11):5583-91. doi: 10.1167/iovs.09-5017 pmid: 20505206
40. Jabbarvand M, Khodaparast M, Jamali A, Ahmadzadeh H, Bordbar S. Changes in the Optical Corneal Densitometry, Visual Acuity, and Refractive Error after the Annular Intracorneal Inlay Implantation. J Curr Ophthalmol. 2021;33(1):23-30. doi: 10.4103/JOCO.JOCO_154_20 pmid: 34084953
41. Abd Elaziz MS, El Saebay Sarhan AR, Ibrahim AM, Elshafy Haggag HA. Anterior Segment Changes After Femtosecond Laser-Assisted Implantation of a 355-Degree Intrastromal Corneal Ring Segment in Advanced Keratoconus. Cornea. 2018;37(11):1438-1443. doi: 10.1097/ICO.0000000000001702 pmid: 30028749
42. Rho CR, Na KS, Yoo YS, Pandey C, Park CW, Joo CK. Changes in anterior and posterior corneal parameters in patients with keratoconus after intrastromal corneal-ring segment implantation. Curr Eye Res. 2013;38(8):843-50. doi: 10.3109/02713683.2013.788723 pmid: 23806046
43. Cankaya AB, Tekin K, Kiziltoprak H, Karahan S, Yilmazbas P. Assessment of corneal backward light scattering in the healthy cornea and factors affecting corneal transparency. Jpn J Ophthalmol. 2018;62(3):335-341. doi: 10.1007/s10384-018-0584-7 pmid: 29549461
44. Fariselli C, Vega-Estrada A, Arnalich-Montiel F, Alio JL. Artificial neural network to guide intracorneal ring segments implantation for keratoconus treatment: a pilot study. Eye Vis (Lond). 2020;7:20. doi: 10.1186/s40662-020-00184-5 pmid: 32292796